JOURNAL OF MATERIALS SCIENCE 37 (2002) 745–751

Oxygen-stabilised partial amorphisation in a $Zr_{50}Cu_{50}$ alloy

Z. Y. LIU
School of Metallurgy and Materials, The University of Birmingham, Edgbaston, Birmingham, B15 2TT, UK

M. AINDOW
Department of Metallurgy and Materials Engineering, Institute of Materials Science, U-136, University of Connecticut, Storrs, CT 06269-3136, USA

J. A. HRILJAC
School of Chemistry, The University of Birmingham, Edgbaston, Birmingham, B15 2TT, UK

I. P. JONES, I. R. HARRIS
School of Metallurgy and Materials, The University of Birmingham, Edgbaston, Birmingham, B15 2TT, UK

Structural transitions on heating a ZrCu martensite prepared by induction melting and subsequent rapid cooling have been investigated by means of differential scanning calorimetry (DSC), electrical resistivity measurements, X-ray diffractometry (XRD) and transmission electron microscopy (TEM). The ZrCu martensite firstly transforms to the ZrCu compound with the B2 structure at around 300°C. Depending upon the annealing temperature, there are two routes for the ZrCu compound to reach equilibrium. By annealing at $T \geq 425$°C, the equilibrium state, i.e. a eutectoid mixture of Zr_7Cu_{10} and Zr_2Cu, is attained directly because the required chemical segregation for the equilibrium phases can be satisfied; alternatively, by annealing at 300°C $< T <$ 425°C, the equilibrium state is reached via another metastable state, an amorphous phase. This is, however, present only locally and contains significant levels of oxygen. A qualitative explanation of the observed structural transitions is given in terms of thermodynamic and kinetic considerations.

1. Introduction

Materials can be rendered amorphous starting from all three phases of matter, viz. vapour, liquid and solid. With reference to the starting state of a material, routes that can produce an amorphous phase hence fall into three broad categories: (1) codeposition from the vapour, (2) quenching from the melt and (3) solid-state reaction. Isothermally annealing thin-multilayered crystalline metals, for example La and Au, at low temperature [1] is one of the several ways of producing an amorphous phase via the last category, i.e., solid-state reaction. In this, the essential feature is that, thermodynamically, interdiffusion of La and Au occurs with a negative heat of mixing which provides the necessary chemical driving force for the amorphisation. Kinetically, due to the different atomic mobilities (the smaller Au atoms are mobile while the larger La ones are essentially immobile) the formation of crystalline intermetallic phases, which have even larger negative heats of formation, can thereby be precluded. Besides the La-Au system, metallic systems consisting of one early transition metal, e.g. Zr, Hf, and one of the late transition metals, e.g. Cu, Co, Ni, Fe have been found to exhibit this behaviour [2].

Our present investigation into amorphization via solid-state reaction in the Zr-Cu system stemmed from the work of Nicholls *et al*. [3]. They found that heating the ZrCu martensite seemed to result in an intermediate amorphous or very fine microcrystalline ZrCu phase before the occurrence of the eutectoid mixture of Zr_7Cu_{10} and Zr_2Cu. Recently, the structural transitions from the martensitic ZrCu phase to the eutectoid mixture have been studied in some detail by the present authors [4]. Annealing the ZrCu martensite at 350°C for 24 hours causes a partial amorphization process; as a result a few amorphous regions can be seen to be surrounded by martensitic ZrCu matrix. These amorphous regions have been found to contain considerable oxygen. This paper reports further studies of the structural transitions, and the partial amorphization process in particular, with the aim of shedding light upon the nature of this process and the formation mechanism for the amorphous phase in the Zr-Cu system in the presence of oxygen.

TABLE I List of the main impurities in the elemental Zr and Cu (in wt ppm)

Elemental Zr	
C	250
Fe	200
N	100
H	10
Hf	2500
Cr	200
O	1000
Zr	Balance
Elemental Cu	
Ag	70
Bi	1
Cr	<1
Mg	1
Na	<1
Pb	2
Sn	1
Al	1
Ca	1
Fe	2
Mn	<1
Ni	2
Si	2
Cu	Balance

2. Experimental procedures

A Zr-50 at.% Cu alloy was synthesised by induction melting of elemental Zr and Cu (purchased from Goodfellow Limited, Cambridge, England; the main impurities are listed in Table I) on a water-cooled copper hearth under a titanium-gettered Ar atmosphere. Ingots were remelted several times to ensure homogeneity. The sequence of structural changes in the as-cast $Zr_{50}Cu_{50}$ specimens on heating was monitored by differential scanning calorimetry (DSC) and electrical resistivity measurements. DSC was carried out in a Netzsch DSC 404C calorimeter under an argon flow of 90 ml/min. The resistivity was measured in vacuum (10^{-3} Pa) by means of a four-point-probe method. Annealing was carried out by sealing the as-cast ingots in silica tubes evacuated to a pressure of approximately 10^{-4} Pa, and then heat treating at 250°C, 300°C, 350°C, 375°C, 400°C, 425°C, 550°C, 650°C and 750°C, respectively for 24 hours followed by quenching into liquid nitrogen. Structural characterisation was performed by X-ray diffractometry (XRD) and transmission electron microscopy (TEM). XRD patterns were collected on the bulk material in reflection geometry using a Bruker D5005 diffractometer equipped with a primary beam Göbel mirror and position sensitive detector. High temperature experiments utilised an Anton Paar HTK 1200 furnace. Specimens suitable for TEM observations were prepared by electropolishing in a solution of 10 vol% nitric acid, 15 vol% glycerine and 75 vol% methanol at −35°C and a voltage of 30 V. TEM specimens were also prepared by the ion-beam milling technique under conditions of 5 kV gun voltage and 1 mA beam current at an incidence angle of 12° (Gatan Duomill). Chemical composition analysis was performed by means of energy dispersive X-ray (EDX). Electron microscopes used in this work were a Philips CM20 and a JEOL FX4000.

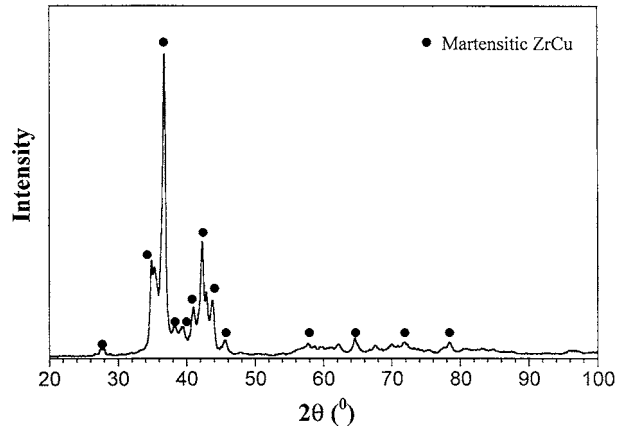

Figure 1 Room temperature XRD pattern of an as-cast $Zr_{50}Cu_{50}$ specimen. All the peaks are indexed according to the monoclinic martensitic ZrCu structure.

3. Results

Fig. 1 is the room temperature XRD pattern of an as-cast $Zr_{50}Cu_{50}$ specimen. In Fig. 1, all the peaks were indexed according to a martensitic structure with lattice parameters $a = 0.6316$ nm, $b = 0.8562$ nm, $c = 0.5331$ nm and $\beta = 105.27°$ [5]. Another previously reported martensitic structure ($a = 0.3278$ nm, $b = 0.4161$ nm, $c = 0.5245$ nm, $\beta = 103.88°$ [5]) was not observed in this work because this structure is only a transition structure [6] and can be removed by remelting. Starting from the martensitic structure, the sequence of structural transitions taking place on heating to 800°C was monitored by DSC and resistivity measurements. As-cast $Zr_{50}Cu_{50}$ specimens were polished mechanically before both experiments but the surfaces of the specimens became dark afterwards. Fig. 2a and b are a DSC trace taken at a heating rate of 10°C/min and a resistivity curve at 5°C/min, respectively. It is evident from Fig. 2 that both DSC and resistivity results reveal the same sequence of structural changes.

Efforts were made to characterise the structures involved in this sequence by employing *in situ* TEM (JEOL FX4000) and high temperature XRD. These failed because, during both examinations, too much oxygen was introduced and the specimens became extensively oxidised. Because of this problem, the structures were characterised by applying TEM at room temperature to the specimens submitted to *ex situ* heat treatments. There is no difference in the microstructure of the *ex situ* heated specimens which were thinned either by electropolishing or by ion-beam milling.

3.1. Transition from the martensitic ZrCu phase to the B2 structure

The room temperature XRD patterns of the specimens annealed below 425°C and subsequently liquid-nitrogen quenched are identical to that of the as-cast specimen, presented in Fig. 1. A bright field TEM image of a specimen annealed at 400°C is shown in Fig. 3. It is characteristic of internally twinned martensite. It appears that the B2 structure obtained at 400°C transforms back to the martensitic ZrCu phase during quenching. This is confirmed by analysing the high temperature

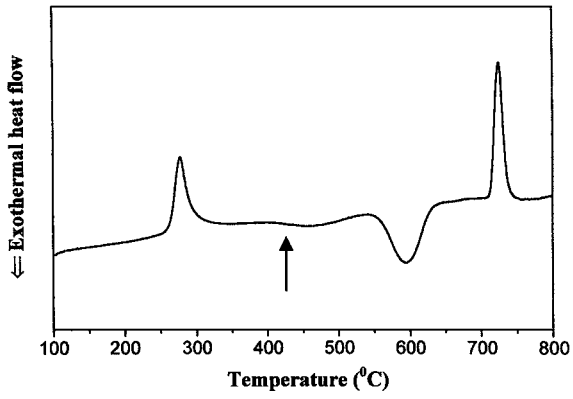

(a)

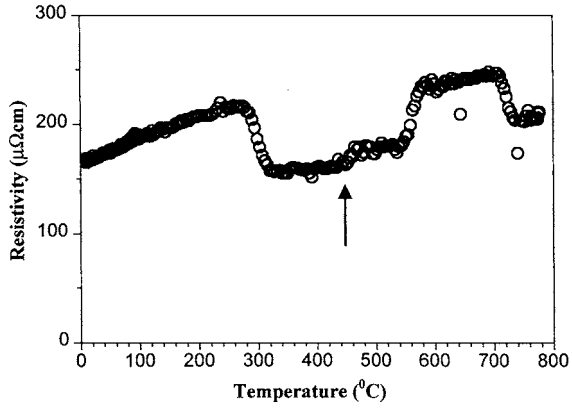

(b)

Figure 2 Sequence of structural changes in as-cast $Zr_{50}Cu_{50}$ monitored by (a) DSC, at a heating rate of 10°C/min and (b) electrical resistivity, at a heating rate of 5°C/min.

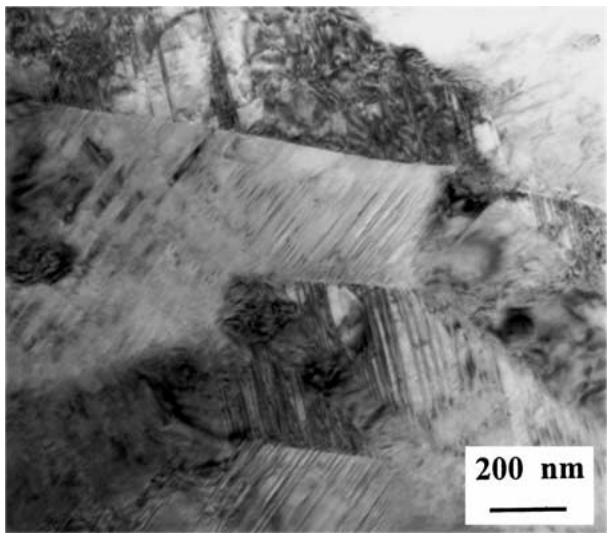

Figure 3 Microstructure of a $Zr_{50}Cu_{50}$ specimen annealed at 400°C in vacuum for 24 hours showing internally twinned martensite.

XRD pattern obtained at 400°C, given in Fig. 4a. It should be noted that the specimen was heated directly to 400°C from room temperature at a rate of 60°C/min. This was to ensure that the dwell time of the specimen at high temperatures was short to reduce oxidation of the specimen, though this is still a serious problem. Whereas some peaks in Fig. 4a cannot be indexed due to oxidation, peaks belonging to the B2 structure can readily be identified. Furthermore, the lattice constant of the B2 structure calculated from the indexed peaks

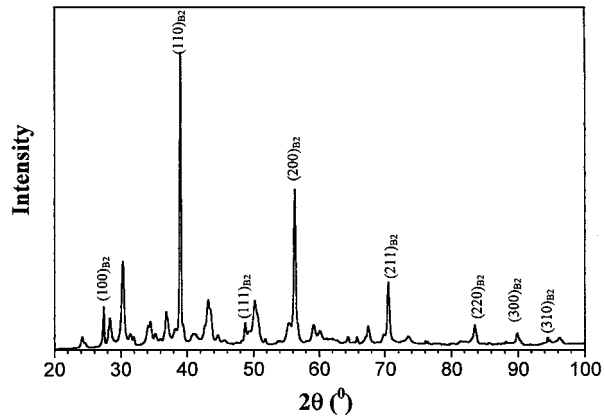

(a)

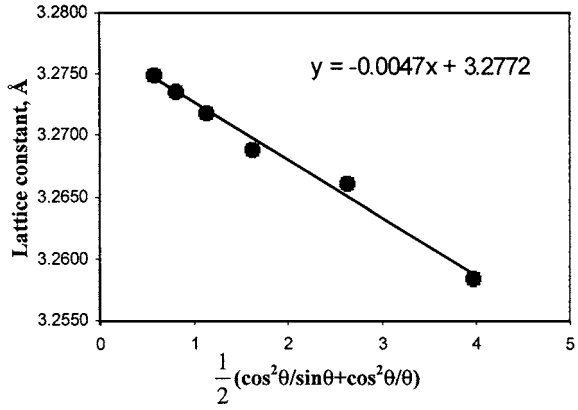

(b)

Figure 4 (a) High temperature XRD pattern of a $Zr_{50}Cu_{50}$ specimen obtained at 500°C and indexed as the B2 structure. The unidentified peaks belong to oxide. (b) Lattice constant of the B2 structure calculated from (a).

is 3.2772 ± 0.0005 Å, as given in Fig. 4b. This value is close to that reported by Carvalho *et al.* [7] and is in good agreement with that of Kneller *et al.* [8]. Accordingly, the endothermic peak in DSC and the fall in resistivity within the temperature range from 280°C to 320°C in Fig. 2 are attributed to the transition from the martensitic ZrCu phase to the B2 structure.

3.2. Eutectoid decomposition

In an attempt to identify the transition corresponding to the exothermic peak in the DSC trace and to the rise in resistivity within the temperature range from 560°C to 640°C in Fig. 2, specimens which had been annealed at 650°C for 24 hours and quenched into liquid nitrogen were examined by room temperature XRD and TEM. Fig. 5a is the XRD pattern and all the peaks in this pattern are ascribable to one of two phases, i.e. Zr_7Cu_{10} and Zr_2Cu. The TEM image shows these two phases adopt a lamellar morphology which is illustrated in Fig. 5b. There is a well defined orientation relationship between these two phases, i.e. $[010]_{Zr_2Cu} \parallel [1\bar{1}0]_{Zr_7Cu_{10}}$; $(001)_{Zr_2Cu} \parallel (110)_{Zr_7Cu_{10}}$ [9]. Based on the present results as well as the phase diagram of the Zr-Cu system [8], the transformation within the temperature range from 560°C to 640°C in Fig. 2 was identified to be the eutectoid decomposition process from which phases Zr_7Cu_{10} and Zr_2Cu were produced.

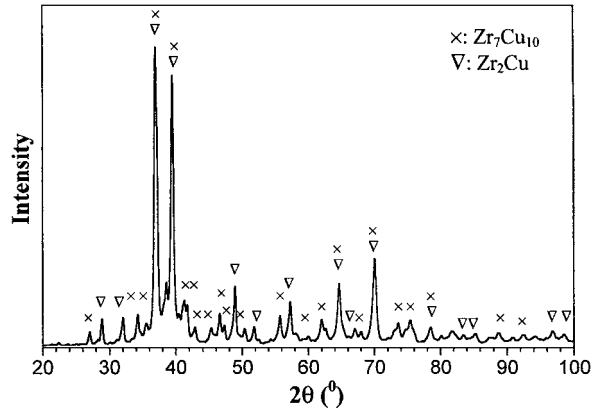

(a)

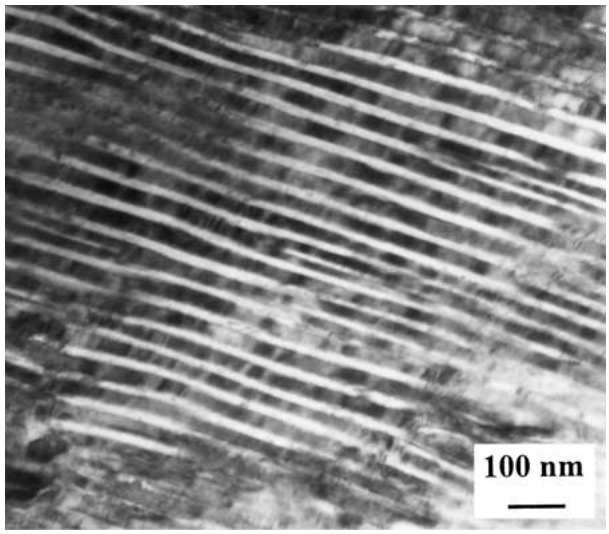

(b)

Figure 5 Room temperature XRD pattern (a) and microstructure (b) of a $Zr_{50}Cu_{50}$ specimen annealed at 650°C in vacuum for 24 hours. The lamellar-type morphology in (b) is made up of the eutectoid mixture Zr_7Cu_{10} (grey) and Zr_2Cu (white).

3.3. Eutectoid recombination

The room temperature XRD and TEM results obtained from specimens annealed at 750°C for 24 hours are the same as those from as-cast specimens. Thus at 750°C the microstructure of the specimen consists of the B2 structure and it transforms to the martensitic ZrCu phase during liquid nitrogen quenching. According to the Zr-Cu phase diagram [8], the eutectoid temperature T_E is 712°C. Therefore, the variations both in the heat flow (the last endothermic peak in the DSC trace) and in the resistivity (the last fall) at about 710°C in Fig. 2 correspond to the eutectoid recombination reaction in which the B2 structure is formed from Zr_7Cu_{10} and Zr_2Cu at T_E.

3.4. Partial amorphisation

Besides the foregoing transitions, there is another, less obvious one, indicated by an arrow in both Fig. 2a and b. The temperature range for this transition is from about 400°C to 540°C. TEM revealed that a few amorphous regions are surrounded by the martensitic ZrCu matrix in specimens annealed at 300°C $< T <$ 425°C but no such phenomenon was found in specimens annealed either below 300°C or above/at 425°C. This partial amorphisation was assumed to be responsible for the variations in both heat flow and resistivity within the temperature range from around 400°C to 540°C in Fig. 2.

Fig. 6 shows a bright field TEM image of a specimen annealed at 350°C for 24 hours and subsequently quenched into liquid nitrogen. It is evident that the amorphous phase did not occur uniformly throughout the whole specimen. Instead, it was distributed randomly in the form of localised regions as represented by 'A', 'B' and 'C' in Fig. 6a. A higher magnification image of region A is presented in Fig. 6b. It is surrounded by internally twinned or heavily dislocated martensite. In some regions of the surrounding martensite, although dislocations are no longer visible, bend contours still exist, providing evidence of crystallinity. Region A exhibits uniform contrast and the selected area electron diffraction (SAD) pattern taken from it is given as an inset. This shows a diffraction halo characteristic of an amorphous phase. Chemical analysis was carried out using EDX fitted to a Philips CM20 TEM. The analysis was applied to region A and showed that it contains significant levels of oxygen. This can clearly be seen from Fig. 7, a composition profile across region A along the straight line in Fig. 6b. Similar results were obtained from regions B and C. Although the amorphous region is thinner (which would cause the soft oxygen signal to rise), the fact that the ZrL/CuK graph (Fig. 7) rises in the same way suggests strongly that the oxygen rise is real.

A survey of the volume fraction of the amorphous phase and its dimensions was made among all the specimens annealed at 300°C $< T <$ 425°C. The volume fraction was estimated roughly with the aid of TEM by measuring the fractional area of the amorphous regions observed in a specimen . In this way the volume fraction was found to be less than 2% for all specimens examined. Since this value is so small, it is difficult to make a comparison among these specimens and to determine at which annealing temperature a specimen contains more amorphous phase. The dimensions of the amorphous phase were measured directly by using the measuring mode within the Philips CM20 TEM. The dimensions thus measured are scattered over a wide range from 0.1 to 0.9 μm. Broadly speaking, however, the dimensions are of the order of 0.2 to 0.6 μm, as shown in Fig. 8.

4. Discussion

Fig. 9 summarises the observed structural transitions on annealing the as-cast ZrCu martensite. The upper temperature limit of the existence of the amorphous phase is 425°C and the lower one is not clearcut because it is difficult to determine the onset temperature due to the very small amount of the amorphous phase. In this situation, the lower temperature limit was assumed to be around 300°C. It is worthwhile noting that the B2 structure transforms back to the martensitic ZrCu on quenching to room temperature.

To understand a solid state transition, it is important to consider both thermodynamics and kinetics. The former determines the driving force for the

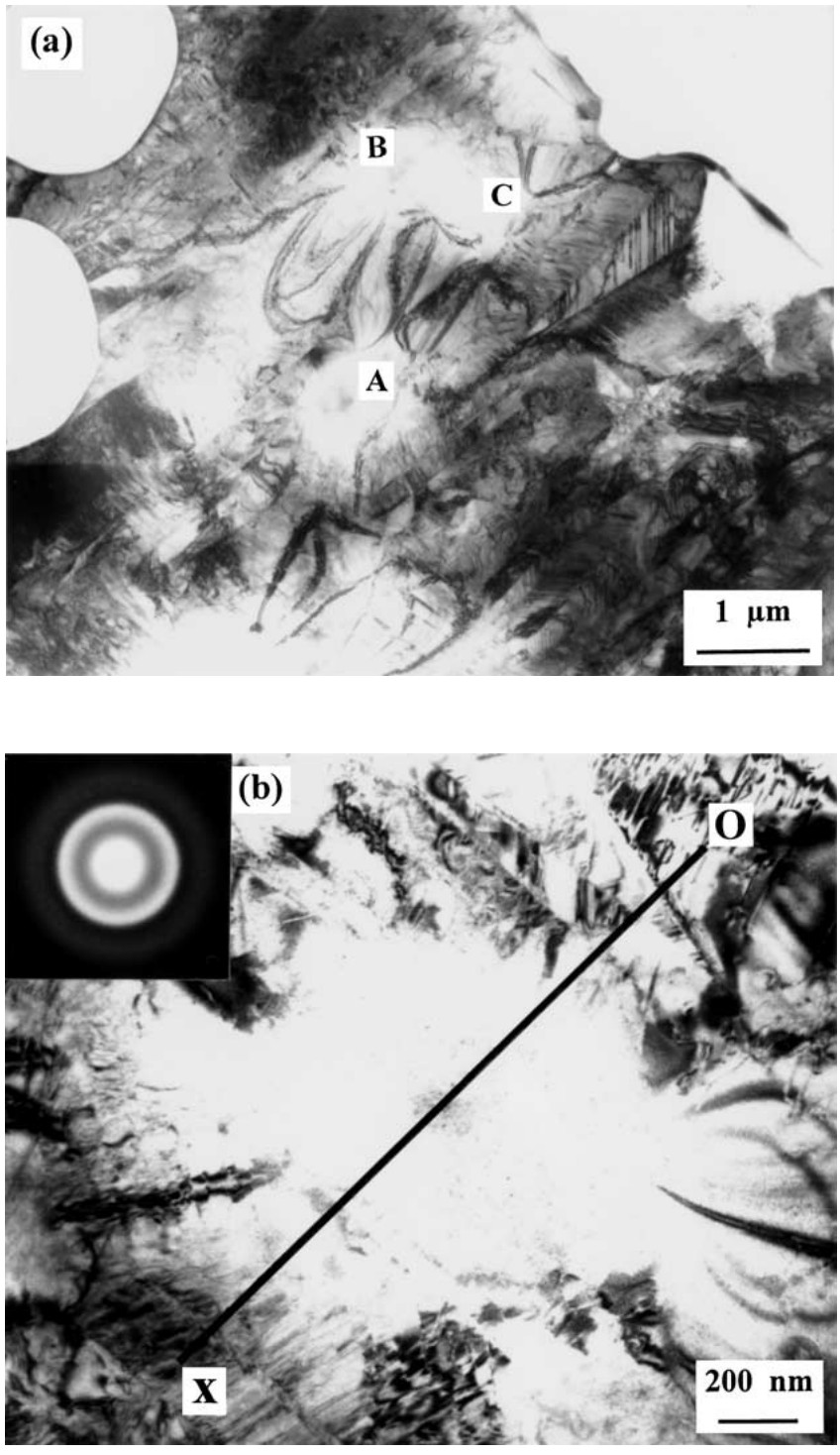

Figure 6 (a): Bright field TEM image of a $Zr_{50}Cu_{50}$ specimen annealed at 350°C in vacuum for 24 hours. The amorphous clusters represented by 'A', 'B' and 'C' are randomly distributed in the martensitic ZrCu matrix; (b): higher magnification image of the amorphous cluster A and its SAD pattern (inset). For chemical analysis along the straight line, see Fig. 7.

transition and the latter governs the rate and therefore the favoured path for the transition. The eutectoid decomposition at $425°C < T < 712°C$ and the recombination at $T > 712°C$ are quite straightforward in a qualitative sense in terms of both thermodynamics and kinetics and no explanation is needed here.

The transition from the martensitic ZrCu phase to the B2 structure at around 300°C is contrary to thermodynamic conditions. According to the Zr-Cu phase diagram [8], the eutectoid decomposition should have occurred. However, kinetics dictates that the first product of a transformation from a metastable system is not necessarily the most stable phase, even though this is associated with the maximum driving force. Precipitation from supersaturated aluminium alloys [10] is a notable example. Provided it is accompanied by a decrease in free enthalpy, a metastable product of lower stability will form preferentially if it can be nucleated at a significantly greater rate. In the present case, the transition occurring at around 300°C is associated with martensitic transformation (MT) [7]. The MT occurs extremely rapidly and, consequently, the transition

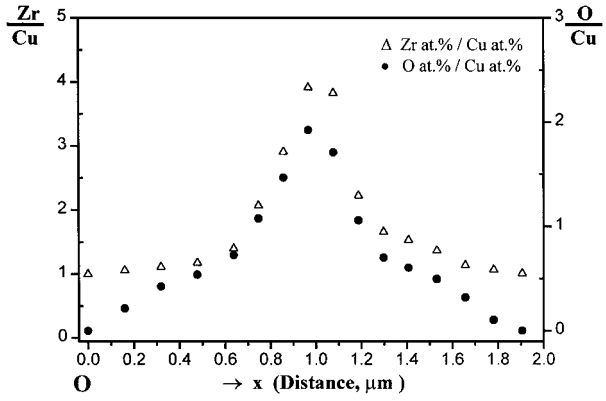

Figure 7 Composition profile across the amorphous cluster A along the straight line as shown in Fig. 6b.

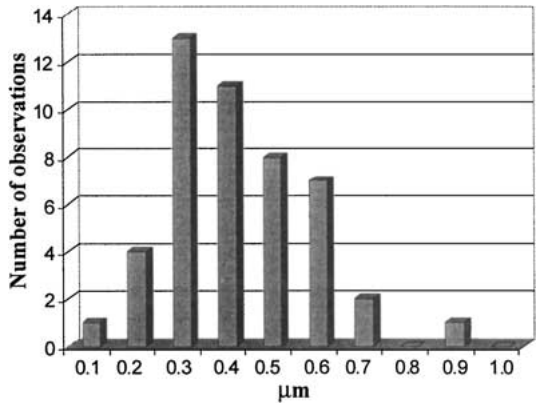

Figure 8 Distribution of dimensions for the amorphous clusters observed in $Zr_{50}Cu_{50}$ specimens annealed below 425°C in vacuum for 24 hours followed by quenching into liquid nitrogen.

from the martensitic ZrCu to the B2 structure is the kinetically favoured route.

The partial amorphisation occurring at $300°C < T < 425°C$ is complicated. The Zr-Cu system is perhaps the best known metal-metal binary system which can be made amorphous over a wide range of composition by rapid quenching [11]. In this, the free enthalpy calculations based on different thermodynamic models [12,13] provide a good understanding of the driving force for the formation of the amorphous phase. Moreover, like the La-Au system, this system can also be made amorphous by a low-temperature reaction of the pure crystalline metals [2]. The driving force for this kind of reaction is a large negative heat of mixing and a detailed description of it was given for the La-Au system [1]. Obviously, the process of the partial amorphisation in the present case is totally different from these cases and hence the driving force for it may also be different.

It was shown earlier that the amorphous phase contains considerable oxygen and it is likely that oxygen plays a significant role in driving the partial amorphisation due to its high affinity for zirconium [14]. If this is the case, the essential factor to be established then is from where does the material absorb oxygen, and when?

There are several possibilities for oxygen to get into the $Zr_{50}Cu_{50}$ alloy and these are as follows:

(a) *From the starting material before melting.* Whereas the solubility of oxygen in fcc Cu is small and reaches a maximum of 0.015 at.% at the eutectoid temperature, that in α-Zr is up to a maximum of 29.8 at.% at 1205°C [15]. The large solubility in the latter case can probably be attributed in part to an unusually strong chemical bonding [14] and in part to the fact that the oxygen atoms are accommodated in the octahedral interstitial sites with very little lattice strain [16]. From Table I, it can be seen that the content of oxygen in elemental Zr is 1000 wt ppm. Therefore, the Zr used in the present study is actually a Zr(O) solid solution.

(b) *From the environment when performing heat treatments or high temperature measurements.* If the sample environment is not completely free of oxygen, oxygen

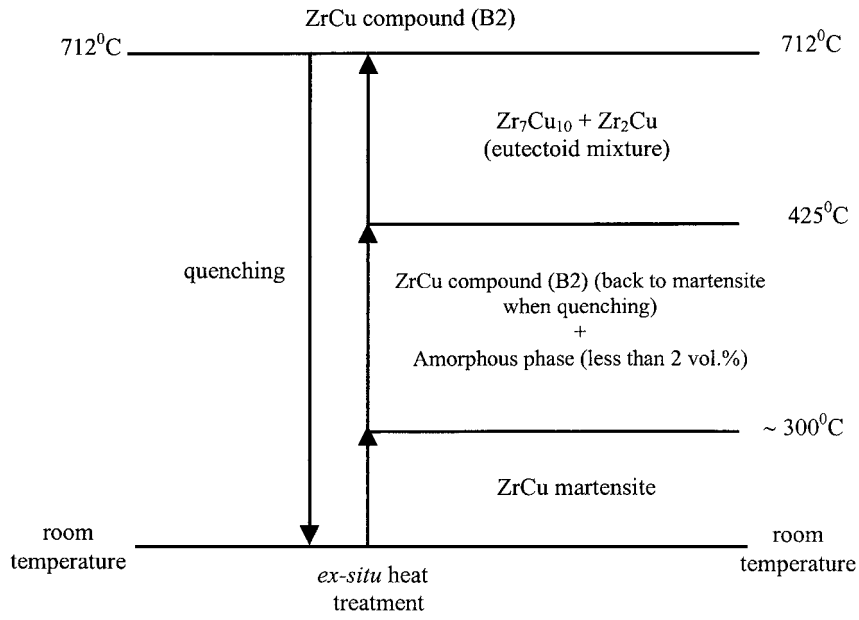

Figure 9 Schematic diagram of the thermal stabilities for the phases in a $Zr_{50}Cu_{50}$ alloy after *ex situ* heat treatments. Consult the text for a more detailed explanation.

contamination will be present throughout the sample preparation and any subsequent experiment. Due to the selective oxidation of zirconium, the sample surface is covered by a thin layer of ZrO_2 when annealing a sample even under a nominally pure argon atmosphere. Further diffusion of oxygen could occur by oxygen homogeneously penetrating the ZrO_2 layer [17].

(c) *From atmosphere during storage or during room temperature experiments*. To date, no information is available on the solubility of oxygen in the martensitic ZrCu. It is possible that oxygen is trapped in the martensite during sample storage or room temperature experiments in air, but there is no visual evidence for such a reaction and this mechanism seems less likely than (a) and (b). At this juncture, no attempt has been made to clarify which of the above possibilities is responsible for the oxygen included in the amorphous phase and it may be that more than one mechanism is involved.

(d) *During specimen thinning*. It is not unknown for electropolishing to create, probably by redeposition, amorphous regions rich in oxygen. Most electropolising, including the one used here are strongly oxidising. We are confident, however, that our amorphous regions are not the result of specimen preparation (i) because ion-beam thinning yielded the same microstructure and (ii) because the presence of the amorphous regions depended on the previous heat treatment.

As when $T < 300^\circ$C, the formation of the stable eutectoid mixture Zr_7Cu_{10} and Zr_2Cu is also frustrated at $300^\circ\text{C} < T < 425^\circ$C since the required chemical segregation via interdiffusion of metal atoms is not sufficient. This provides the metastable B2 structure with the kinetic possibility of transforming into a metastable phase in order to decrease the free enthalpy and this takes the form of oxygen-stabilised amorphous regions.

How does the oxygen play a role in driving the partial amorphisation? Knowing that oxygen is present in the $Zr_{50}Cu_{50}$ alloy, it can be assumed that no oxide (stable or not) is formed in the first place. This is a reasonable assumption since no oxide has been found in the specimens. The partial amorphisation occurring during annealing can therefore be regarded as a precursor to the precipitation of a discrete oxide (probably ZrO_2). The glassy state can be attributed to a change to covalency in the local bonding due to the presence of the oxygen atoms.

In cases when both thermodynamic and kinetic conditions can be readily satisfied, e.g. *ex situ* heat treatment at $T > 425^\circ$C, oxygen does not appear to play a significant role and the $Zr_{50}Cu_{50}$ alloy transforms fully to the eutectoid mixture even in the previously amorphous regions.

It will be interesting to see if complete bulk amorphisation can be achieved by increasing the overall oxygen content.

5. Conclusions

Our investigation reveals a sequence of structural transitions in a ZrCu martensite on heating from room temperature to 800°C: Martensitic ZrCu $\rightarrow$ B2 $\rightarrow$ Amorphous phase (partial) $\rightarrow Zr_7Cu_{10} + Zr_2Cu$ (eutectoid) $\rightarrow$ B2. The.amorphous phase has been found to contain significant levels of oxygen with respect to its surrounding martensitic ZrCu matrix. The partial amorphisation is interpreted as a pre-precipitation phenomenon of an oxide (probably ZrO_2) and the covalent character of local bonding.

Acknowledgements

The authors are much obliged to H. Evans and I. T. H. Chang for helpful discussions. An anonymous referee made some very helpful and constructive suggestions which significantly improved the paper. Financial assistance from the ORS Scheme and the School of Metallurgy and Materials at The University of Birmingham is gratefully acknowledged (ZYL). The XRD equipment was purchased with funding provided by the EPSRC.

References

1. R. B. SCHWARZ and W. L. JOHNSON, *Phys. Rev. Lett.* **51** (1983) 415.
2. W. L. JOHNSON, *Progr. Mater. Sci.* **30** (1986) 81.
3. A. W. NICHOLLS, I. R. HARRIS and W. MANGEN, *J. Mater. Sci. Lett.* **5** (1986) 217.
4. Z. Y. LIU, M. AINDOW, J. A. HRILJAC, I. P. JONES and I. R. HARRIS, *Mater. Sci. Forum* **360–362** (2001) 223.
5. D. SCHRYVERS, G. S. FIRSTOV, J. W. SEO, J. VAN HUMBEECK and YU. N. KOVAL, *Scripta Mater.* **36** (1997) 1119.
6. J. W. SEO and D. SCHRYVERS, *Acta Mater.* **46** (1998) 1165.
7. E. M. CARVALHO and I. R. HARRIS, *J. Mater. Sci.* **15** (1980) 1224.
8. E. KNELLER, Y. KNAN and URSULA GORRES, *Z. Metallkde.* **77** (1986) 43.
9. Z. Y. LIU, M. AINDOW, J. A. HRILJAC, I. P. JONES and I. R. HARRIS, *J. Mater. Sci. Lett.* **20** (2001) 543.
10. H. K. HARDY and T. J. HEAL, "The Mechanism of Phase Transformations in Metals," Monograph and Report Series No. 18 (The Institute of Metals, London, 1956) p.1.
11. R. RAY, B. C. GIESSEN and N. J. GRANT, *Scripta Metall. Mater.* **2** (1968) 357.
12. N. SAUNDERS and A. P. MIODOWNIK, *J. Mater. Res.* **1** (1986) 38.
13. R. BORMANN, F. GARTNER and F. HAIDER, *Mater. Sci. Engr.* **97** (1988) 79.
14. I. BARIN and O. KNACKE, "Thermochemical Properties of Inorganic Substances" (Springer, Berlin, 1973).
15. T. B. MASSALSKI, "Binary Alloy Phase Diagrams," 2nd. ed. (ASM International, 1990) p. 1446 and 2940.
16. G. V. KIDSON, "Diffusion in Body-Centered Cubic Metals" (American Society for Metals, Metals Park, OH, 1965) p. 329.
17. D. QUATAERT and F. COEN-PORISINI, *J. Nucl. Mater.* **36** (1970) 20.

Received 2 February
and accepted 2 October 2001